A Quasi-Generalized-Coordinate Approach for Numerical Simulation of Complex Flows

Donghyun You[1]
Center for Turbulence Research,
Stanford University,
Stanford, CA 94305
e-mail: dyou@stanford.edu

Meng Wang
Department of Mechanical and Aerospace Engineering,
George Washington University,
Washington, DC 20052 and
Department of Aerospace and Mechanical Engineering,
University of Notre Dame,
Notre Dame, IN 46556

Rajat Mittal
Department of Mechanical and Aerospace Engineering,
George Washington University,
Washington, DC 20052

Parviz Moin
Center for Turbulence Research,
Stanford University,
Stanford, CA 94305

A novel structured grid approach which provides an efficient way of treating a class of complex geometries is proposed. The incompressible Navier-Stokes equations are formulated in a two-dimensional, generalized curvilinear coordinate system complemented by a third quasi-curvilinear coordinate. By keeping all two-dimensional planes defined by constant third coordinate values parallel to one another, the proposed approach significantly reduces the memory requirement in fully three-dimensional geometries, and makes the computation more cost effective. The formulation can be easily adapted to an existing flow solver based on a two-dimensional generalized coordinate system coupled with a Cartesian third direction, with only a small increase in computational cost. The feasibility and efficiency of the present method have been assessed in a simulation of flow over a tapered cylinder.
[DOI: 10.1115/1.2354533]

1 Introduction

In large-eddy simulation (LES) of flows in complex geometries, the generation of a high-quality mesh and the large memory requirement for the metric quantities of coordinate transformation are often major obstacles, when a three-dimensional structured, body-fitted mesh is employed. The problem is particularly severe for flow solvers employing the staggered mesh arrangement, which is strongly preferred in nondissipative LES codes for stability and discrete energy conservation (e.g. [1,2]). For instance, at least 80 (eight positions with ten variables (metric coefficients plus Jacobian) per mesh element) three-dimensional arrays are required, compared to ten three-dimensional arrays for collocated meshes. This makes LES employing a staggered grid impractical on large grids. In addition, the increase of partial derivative terms in the transformed governing equations cause a significant increase in computational cost.

On the other hand, many geometries in engineering and scientific applications can be handled using a two-dimensional curvilinear mesh with mild variations along the remaining third direction. Frequently observed variations are shift, rotation, magnification/contraction, and skewing of the curvilinear plane along a direction perpendicular to that plane. The airplane wing is an example of the shift and contraction of the airfoil section, and the blades in an axial compressor or turbine are observed to be twisted along the radial direction while maintaining the blade section profile.

The objective of this study is to exploit these geometric simplifications in the design of a numerical method, which can be applicable to a wide class of problems while minimizing the memory requirement and computational cost. To this end, a formulation of incompressible Navier-Stokes equations based on a "quasi-generalized" coordinate system is proposed. This coordinate system consists of two generalized curvilinear coordinates and a third quasi-curvilinear coordinate. By keeping all two-dimensional planes defined by constant third coordinate values parallel to one another, one can efficiently treat a wide class of fully three-dimensional geometries, and, at the same time, avoid the large memory requirement and high-computational cost associated with a fully generalized coordinate transformation, especially when a staggered grid is used for stability of nondissipative large-eddy simulation. In nondissipative LES, aliasing errors are controlled by enforcing kinetic energy conservation in contrast to the LES techniques employing dissipative upwind-biased schemes or to the implicit LES [3] which relies on a high-order spatial filter in lieu of a subgrid-scale model. The nondissipative feature was proven to be important for successful LES of turbulent flows [1,4] and it has been shown that better stability of the nondissipative algorithm is achievable by utilizing a staggered mesh [5,6].

A number of structured grid approaches have been proposed to handle mildly three-dimensional flow configurations. For instance, You et al. [5] and Tang et al. [7] proposed methods employing a three-dimensional grid which is generated by either merely translating or rotating a whole two-dimensional curvilinear grid along the remaining third coordinate. The present method significantly differs from the previous methods [5,7] in that it allows more general variations of a two-dimensional base grid along the remaining third coordinate, and therefore, can be utilized to confront problems involving a step further complex geometries.

The incompressible Navier-Stokes equations are transformed to a quasi-generalized coordinate system in Sec. 2. Then, in Sec. 3, formulas for some examples of geometric variations and their applicability are given. In Sec. 4, an implementation of the present formulation is evaluated by considering the flow over a tapered circular cylinder, and this is followed by a brief summary in Sec. 5.

2 Transformation of Governing Equations

The incompressible Navier-Stokes equations based on Cartesian coordinates are as follows:

$$\frac{\partial u_i}{\partial t} + \frac{\partial}{\partial x_j} u_i u_j = -\frac{\partial p}{\partial x_i} + \frac{1}{\mathrm{Re}} \frac{\partial}{\partial x_j} \frac{\partial u_i}{\partial x_j} \tag{1}$$

$$\frac{\partial u_i}{\partial x_i} = 0 \tag{2}$$

All the coordinate variables, velocity components, and pressure are nondimensionalized by a length scale L, reference velocity U_{ref}, and ρU_{ref}^2, respectively. The time is normalized by L/U_{ref}.

Equations (1) and (2) can be rewritten in the conservative form in a generalized coordinate system as

[1]Corresponding author.

Contributed by the Fluids Engineering Division of ASME for publication in the JOURNAL OF FLUIDS ENGINEERING. Manuscript received October 11, 2005; final manuscript received April 11, 2006. Assoc. Editor: Surya P. Vanka.

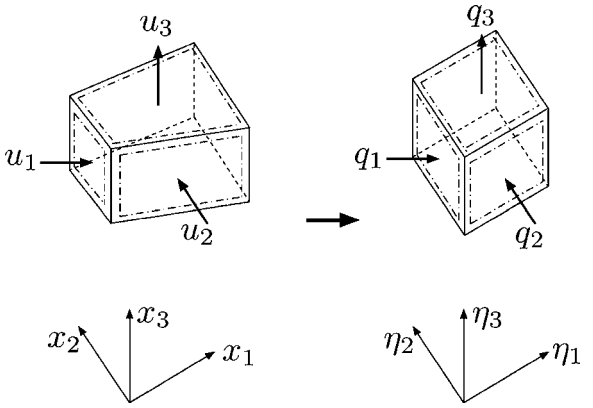

Fig. 1 Schematic diagram of coordinate transformation from Cartesian coordinates to curvilinear coordinates. Planes perpendicular to η^3 are required to be parallel in the quasi-generalized coordinates.

$$\frac{\partial q^i}{\partial t} = -N^i(\mathbf{q}) - G^i(p) + L^i(\mathbf{q}) \tag{3}$$

$$D^i q^i = 0 \tag{4}$$

where $\mathbf{q}=(q^1,q^2,q^3)$, N^i is the nonlinear convection term, $G^i(p)$ is the pressure gradient term, and L^i represents the diffusion term. D^i denotes the divergence operator. A transformation to generalized coordinates is introduced in Fig. 1 as

$$(x_1,x_2,x_3;u_1,u_2,u_3) \rightarrow (\eta^1,\eta^2,\eta^3;q^1,q^2,q^3) \tag{5}$$

The variable q^i is the volume flux across the faces of the cells, which is equivalent to the contravariant velocity components on a staggered grid multiplied by the Jacobian of the coordinate transformation. Then, the terms in Eq. (3) are expressed in generalized coordinates as

$$N^i(\mathbf{q}) = \frac{1}{J}\gamma_m^j \frac{\partial}{\partial \eta^j}\frac{1}{J}c_k^m q^k q^j \tag{6}$$

$$G^i(p) = \alpha^{ij}\frac{\partial p}{\partial \eta^j} \tag{7}$$

$$L^i(\mathbf{q}) = \frac{1}{J}\gamma_m^j \frac{\partial}{\partial \eta^k}\alpha^{kj}\frac{1}{\mathrm{Re}}\frac{\partial}{\partial \eta^j}\frac{1}{J}c_l^m q^l \tag{8}$$

where

$$q^j = \gamma_k^j u_k, \quad c_k^j = \partial x_j/\partial \eta^k, \quad \gamma_k^j = J(c_j^k)^{-1}, \quad \alpha^{jk} = J(c_j^m c_k^m)^{-1}$$
$$\text{and} \quad J = (\|c_j^m c_k^m\|)^{1/2} \quad \text{for } j,k,l,m,n = 1,2,3$$

When the fully three-dimensional curvilinear coordinate system is used, the large number of partial derivative terms in the transformed governing equations and the required memory for three-dimensional metric coefficients and Jacobians severely limit the computation to a relatively small number of mesh points. Here, we propose an approach which drastically reduces the memory requirement and computational cost. This is done by imposing a constraint which requires the planes defined by constant values of one coordinate (η^3 in the present formulation) to be parallel to one another. This results in $c_1^3=c_2^3=\gamma_1^3=\gamma_2^3=0$. With these vanishing metric quantities, a significant reduction of derivative terms in the transformed Navier-Stokes equations, compared to the equations in a fully three-dimensional generalized curvilinear coordinate system, is obtained:

$$\begin{aligned}\frac{\partial q^i}{\partial t} = &-\frac{1}{J}\gamma_1^j\frac{\partial}{\partial \eta^j}\frac{1}{J}c_k^1 q^k q^j - \frac{1}{J}\gamma_2^j\frac{\partial}{\partial \eta^j}\frac{1}{J}c_k^2 q^k q^j \\ &-\frac{1}{J}\gamma_3^j\frac{\partial}{\partial \eta^j}\frac{1}{J}\Big(\underbrace{c_1^3 q^1 + c_2^3 q^2}_{=0} + c_3^3 q^3\Big)q^j + \alpha^{ij}\frac{\partial p}{\partial \eta^j} \\ &+\frac{1}{J}\gamma_1^j\frac{\partial}{\partial \eta^k}\alpha^{kj}\frac{1}{\mathrm{Re}}\frac{\partial}{\partial \eta^j}\frac{1}{J}c_l^1 q^l + \frac{1}{J}\gamma_2^j\frac{\partial}{\partial \eta^k}\alpha^{kj}\frac{1}{\mathrm{Re}}\frac{\partial}{\partial \eta^j}\frac{1}{J}c_l^2 q^l \\ &+\frac{1}{J}\gamma_3^j\frac{\partial}{\partial \eta^k}\alpha^{kj}\frac{1}{\mathrm{Re}}\frac{\partial}{\partial \eta^j}\frac{1}{J}\Big(\underbrace{c_1^3 q^1 + c_2^3 q^2}_{=0} + c_3^3 q^3\Big)\end{aligned} \tag{9}$$

for $i=1,2$, and $j,k,l=1,2,3$, and

$$\begin{aligned}\frac{\partial q^3}{\partial t} = &\underbrace{-\frac{1}{J}\gamma_1^3\frac{\partial}{\partial \eta^j}\frac{1}{J}c_k^1 q^k q^j}_{=0} \underbrace{-\frac{1}{J}\gamma_2^3\frac{\partial}{\partial \eta^j}\frac{1}{J}c_k^2 q^k q^j}_{=0} \\ &-\frac{1}{J}\gamma_3^3\frac{\partial}{\partial \eta^j}\frac{1}{J}\Big(\underbrace{c_1^3 q^1 + c_2^3 q^2}_{=0} + c_3^3 q^3\Big)q^j + \alpha^{3j}\frac{\partial p}{\partial \eta^j} \\ &\underbrace{+\frac{1}{J}\gamma_1^3\frac{\partial}{\partial \eta^k}\alpha^{kj}\frac{1}{\mathrm{Re}}\frac{\partial}{\partial \eta^j}\frac{1}{J}c_l^1 q^l}_{=0} + \underbrace{\frac{1}{J}\gamma_2^3\frac{\partial}{\partial \eta^k}\alpha^{kj}\frac{1}{\mathrm{Re}}\frac{\partial}{\partial \eta^j}\frac{1}{J}c_l^2 q^l}_{=0} \\ &+\frac{1}{J}\gamma_3^3\frac{\partial}{\partial \eta^k}\alpha^{kj}\frac{1}{\mathrm{Re}}\frac{\partial}{\partial \eta^j}\frac{1}{J}\Big(\underbrace{c_1^3 q^1 + c_2^3 q^2}_{=0} + c_3^3 q^3\Big),\end{aligned}$$
$$\text{for } j,k,l = 1,2,3 \tag{10}$$

The total number of surviving derivative terms is only about one half of that in the fully generalized curvilinear coordinate system.

Compared to the formulation with two-dimensional generalized curvilinear coordinates and a nonuniform Cartesian third direction (e.g. [5]), the above formulation which allows the third coordinate to be curvilinear does not change the computational cost significantly. For a numerical algorithm based on a fractional-step method [8], the computational cost is dominated by the inversions of factored matrices and multigrid operations for solving the pressure Poisson equation, which are not much altered by this generalization.

The three-dimensional metric coefficients in the quasi-generalized coordinates can be expressed as products of metric coefficients in a two-dimensional plane and one-dimensional functions along the third direction, with decoupled Jacobians $J=(c_1^1c_2^2-c_2^1c_1^2)^{1/2}c_3^3$. These decoupled metric coefficients and Jacobians, with variations of the plane mesh along the perpendicular third direction as exemplified in the following section, result in a significant reduction of required memory.

3 Plane Variations and Metric Coefficients

In this section, we present several examples of grid topology in which variations along one direction are given by an algebraic relationship. Note that nonalgebraic variations are also allowed in the present formulation, as long as the mesh planes perpendicular to that direction are parallel to one another. In addition, more flexibility in the geometry can be achieved using a combination of these variations.

(*a*) Shift (Fig. 2(*a*))

$$\begin{cases} x_{1_{i,j,k}} = x_{1_{i,j,1}} + x_{1_k}^s \\ x_{2_{i,j,k}} = x_{2_{i,j,1}} + x_{2_k}^s \end{cases}$$

(*b*) Magnification/Contraction (Fig. 2(*b*))

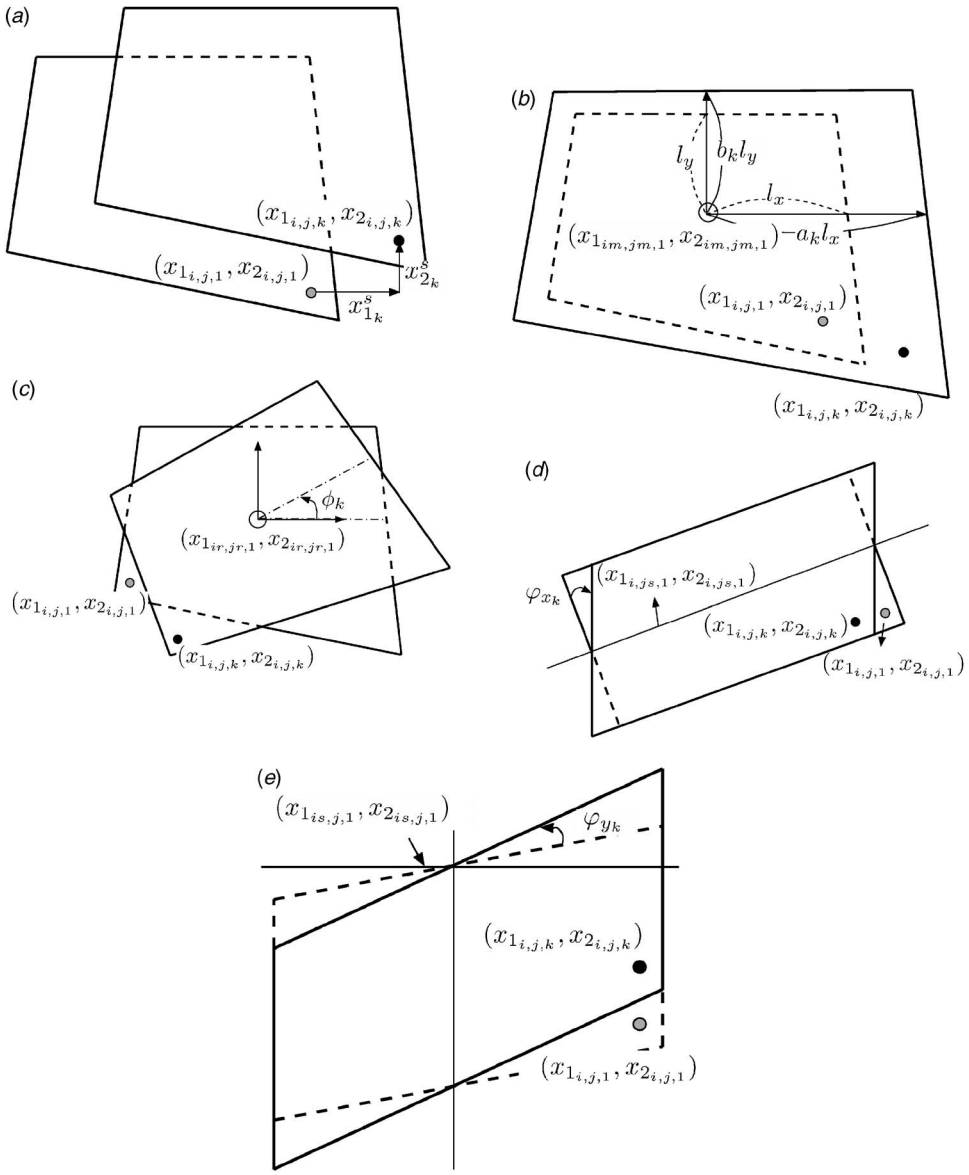

Fig. 2 Examples of algebraic functions used in the proposed transformation: (*a*) shift; (*b*) magnification/contraction; (*c*) rotation; (*d*) skewing to x_1 direction; (*e*) skewing to x_2 direction

$$\begin{cases} x1_{i,j,k} = a_k(x1_{i,j,1} - x1_{im,jm,1}) + x1_{im,jm,1} \\ x2_{i,j,k} = b_k(x2_{i,j,1} - x2_{im,jm,1}) + x2_{im,jm,1} \end{cases}$$

(*c*) Rotation (Fig. 2(*c*))

$$\begin{cases} x1_{i,j,k} = \cos\phi_k(x1_{i,j,1} - x1_{ir,jr,1}) - \sin\phi_k(x2_{i,j,1} - x2_{ir,jr,1}) + x1_{ir,jr,1} \\ x2_{i,j,k} = \sin\phi_k(x1_{i,j,1} - x1_{ir,jr,1}) + \cos\phi_k(x2_{i,j,1} - x2_{ir,jr,1}) + x2_{ir,jr,1} \end{cases}$$

(*d*) Skewing to x_1 direction (Fig. 2(*d*))

$$\begin{cases} x1_{i,j,k} = (x2_{i,j,1} - x2_{i,js,1})\tan^2\varphi_{x_k} + x1_{i,j,1} \\ x2_{i,j,k} = (x2_{i,j,1} - x2_{i,js,1})(1 + \tan^2\varphi_{x_k}) + x2_{i,js,1} \end{cases}$$

(*e*) Skewing to x_2 direction (Fig. 2(*e*))

$$\begin{cases} x1_{i,j,k} = x1_{i,j,1} \\ x2_{i,j,k} = (x1_{i,j,1} - x1_{is,j,1})\tan\varphi_{y_k} + x2_{i,j,1} \end{cases}$$

In the formulas (*a*)–(*e*), $x^s_{1(2)_k}$ is the amount of shift in the $x_1(x_2)$ direction. $x1(2)_{im,jm,1}$, $x1(2)_{ir,jr,1}$, $x2_{i,js,1}$, and $x1_{is,j,1}$ denote reference points for magnification, rotation, and skewing variations in x_1 and x_2 directions, respectively. a_k and b_k are the magnification/contraction factors in x_1 and x_2 directions, while ϕ_k, φ_{x_k}, and φ_{y_k} are the rotation and skewing angles. Additional formulas can be derived to meet other geometric need.

These algebraic variations, as well as combinations of the variations, result in not only geometric flexibility but also decoupled metric coefficients. Any metric coefficients and Jacobians can be expressed as products of those for the base grid at $k=1$ and variational functions along the k direction. This results in a great reduction of computational memory requirements with a negligible increase in computational operations.

Figures 3 and 4 are examples of the geometries which can be represented using the present formulation. Figure 3 shows a compressor blade which is twisted along the blade span while the blade cross-sectional profile is maintained. For this geometry, the base mesh is rotated and skewed along the blade wall normal direction with angles of up to 30 deg, and the skewing allows a periodic boundary condition to be applied in that direction in a

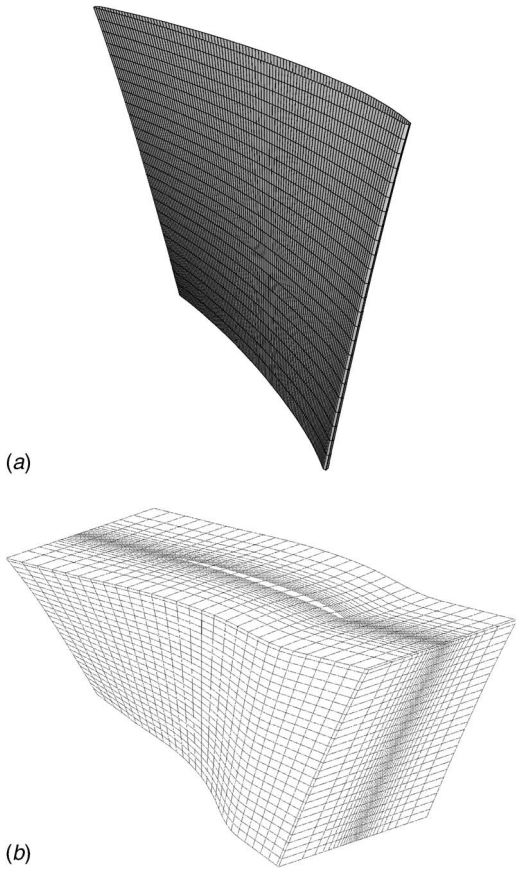

Fig. 3 A twisted compressor blade generated by mesh rotation and skewing: (*a*) compressor blade; (*b*) mesh around the blade

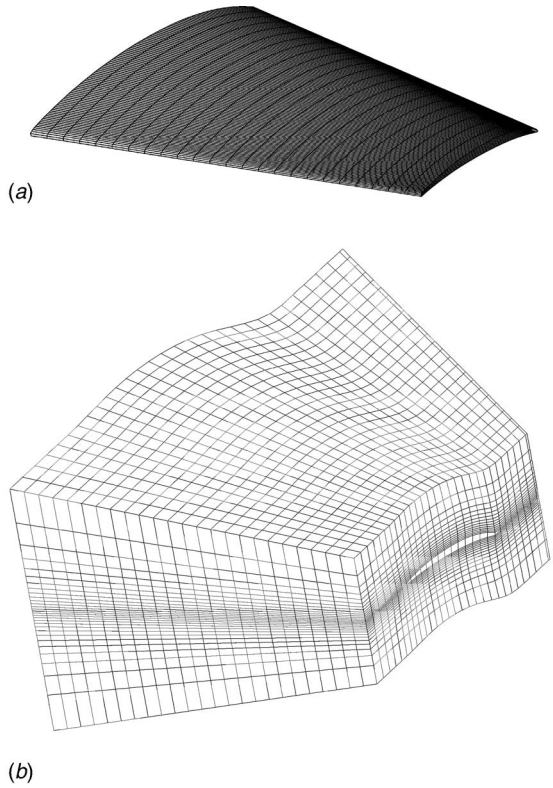

Fig. 4 An airplane wing generated by contraction and shift: (*a*) airplane wing; (*b*) mesh around the wing

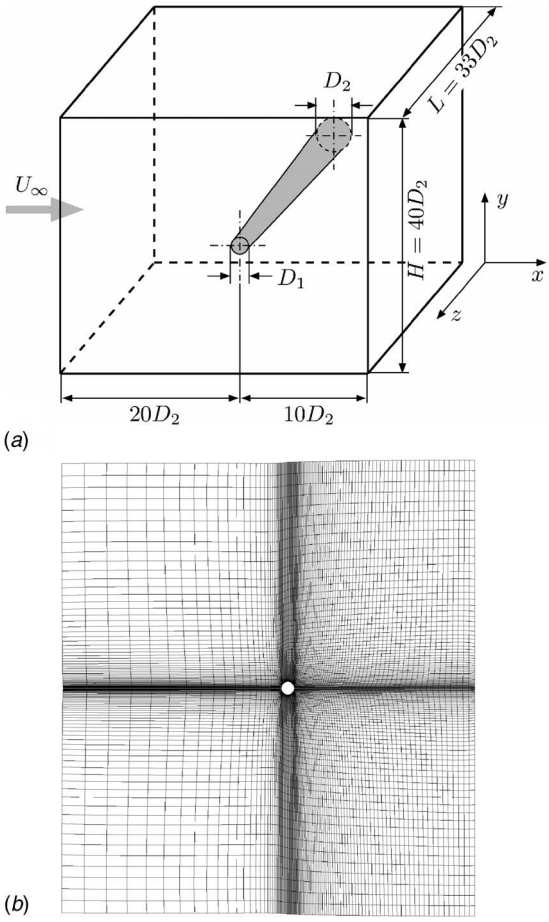

Fig. 5 (*a*) Flow configuration and computational domain, and (*b*) computational grid in a base *x-y* plane used for numerical simulation of flow over a tapered circular cylinder

simulation of flow in a blade passage. An airplane wing can be meshed by contraction and shift operations of the base grid, as shown in Fig. 4. The present approach can also be employed for internal flow configurations such as a pipe and a diffuser whose cross sections vary along the streamwise direction.

Enhanced geometric flexibility can be achieved by combining partially or approximately body-fitted meshes with an immersed boundary method [9,10]. This method has been successfully applied to the rotor tip-clearance flow found in axial turbomachines [5].

4 Implementation and Evaluation

Numerical simulation of vortex shedding behind a linearly tapered cylinder is performed to evaluate the present methodology and implementation. The configuration, shown in Fig. 5(*a*), is the same as that studied experimentally by Piccirillo and Van Atta [11]. The taper ratio, $R_T = L/(D_2 - D_1)$, is set to 50, where L is the cylinder length, and D_1 and D_2 are the diameters of the small and large ends of the cylinder, respectively. The Reynolds numbers based on the diameters and freestream velocity are 60 and 180 at the small and large ends, respectively.

A staggered grid arrangement is employed with the base grid of 257×257 mesh points which is shown in Fig. 5(*b*), and parallel mesh planes are generated along the perpendicular spanwise direction by contraction and expansion operations. Thirty three points are allocated uniformly along the span. A uniform laminar inflow is used and convective and no-stress boundary conditions are employed at the exit and each side wall, respectively. The use

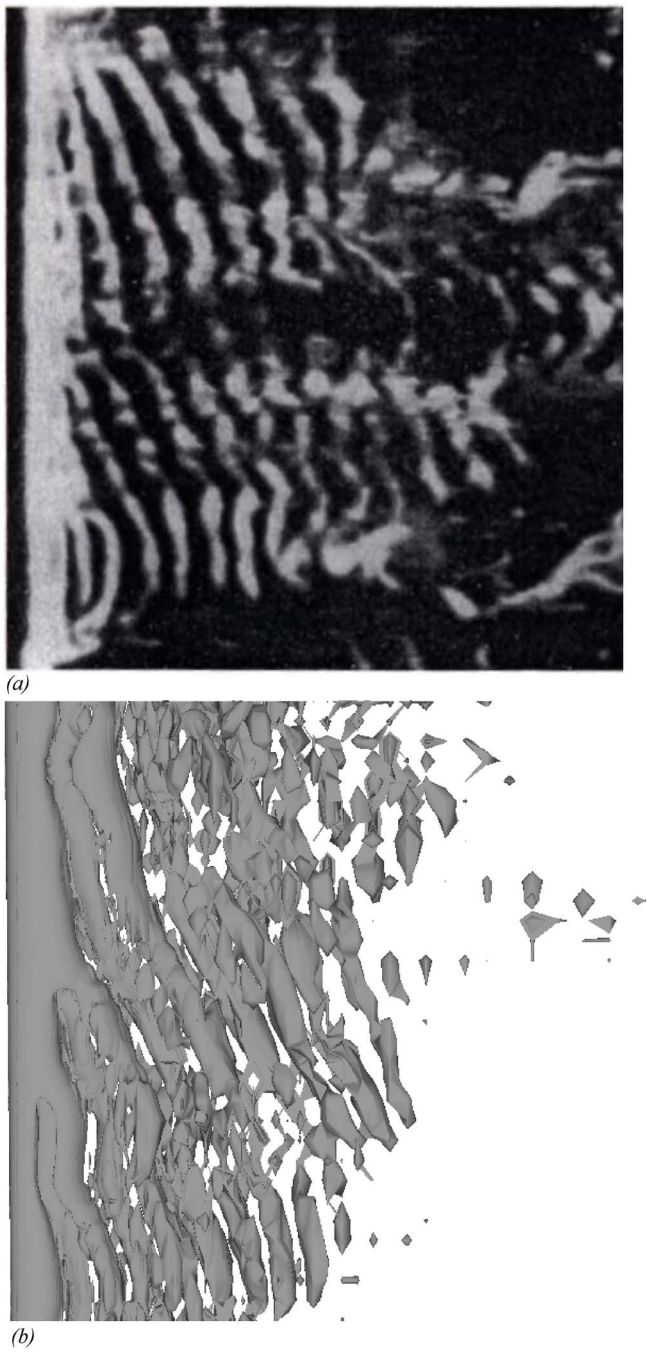

Fig. 6 Instantaneous vortical structures behind a tapered circular cylinder: (*a*) water tunnel flow visualization [11]; (*b*) λ_2 vortex identification from computational results

of a no-stress boundary condition at each side wall can be justified from the experimental observation that the vortex shedding of the flow is largely unaffected by end conditions [11]. About 110 s on 4 CPUs of SGI Origin 300 are used per time step, and this is only about 10% more than that measured by the solver based on the two-dimensional generalized curvilinear coordinate coupled with a straight third direction and with the same number of mesh points.

Figure 6 shows snapshots of instantaneous vortical structures behind the tapered cylinder observed in both the experiment [11] and the present numerical simulation. The oblique vortex shedding is a hallmark of this flow observed experimentally, and the present numerical approach is shown to capture this phenomenon.

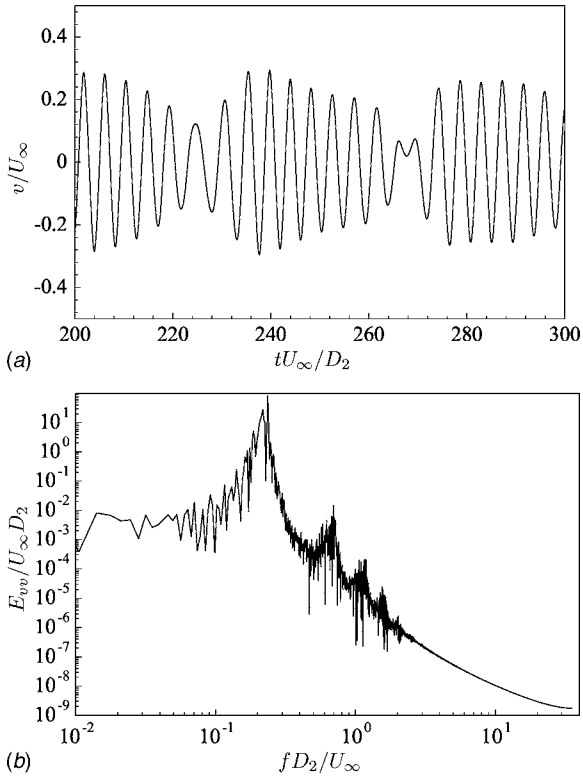

Fig. 7 (*a*) Time history and (*b*) frequency energy spectrum of the vertical velocity at $x/D_2=1$, $y/D_2=0$, $z/D_2=13.5$

In contrast to the laminar vortex shedding observed behind a straight cylinder, phase differences of the vortex shedding along the spanwise direction is clearly observed, and this complicates the downstream vortical structures. This phase difference accelerates the decay of downstream vortices due to enhanced mixing.

Figure 7 shows a typical velocity time history and its autospectrum as a function of nondimensional frequency. The signal represents the velocity at a near-wake position $x/D_2=1$, $y/D_2=0$, and $z/D_2=13.5$. The Strouhal number of vortex shedding at this location is 0.203, which in good agreement with the experimental result ($fD_2/U_\infty=0.204$) of Piccirillo and Van Atta [11].

5 Summary

The incompressible Navier-Stokes equations have been formulated in a two-dimensional, generalized curvilinear coordinate system complemented by a third quasi-curvilinear coordinate. By requiring all the two-dimensional planes to be parallel in the perpendicular direction, the proposed approach makes structured-mesh computation more affordable in fully three-dimensional geometries, in terms of both memory and CPU cost. In particular, it alleviates the huge memory requirement for metric coefficients and Jacobians by eliminating the need to save them as three-dimensional quantities. This feature is especially important when a staggered grid is used for stability of nondissipative large-eddy simulation. The formulation can be easily adapted to an existing solver based on a two-dimensional generalized coordinate system coupled with a Cartesian third direction, with only a small increase in computational cost. Furthermore, the present formulation can be extended to cylindrical (spherical) based coordinates by keeping the axial-circumferential (azimuthal-zenithal) planes parallel to one another in the radial direction.

Acknowledgment

The authors acknowledge the support of the Office of Naval Research under Grant No. N00014-99-1-0389 with Ki-Han Kim

as program manager. Computer time was provided by the Challenge Project Grant C82 from the U.S. Department of Defense High-Performance Computing Modernization Program (HPCMP) through Army Research Laboratory (ARL) Major Shared Resource Center.

References

[1] Mittal, R., and Moin, P., 1997, "Suitability of Upwind-Biased Schemes for Large-Eddy Simulation of Turbulent Flows," AIAA J., **35**(8), pp. 1415–1417.
[2] Nagarajan, S., Lele, S. K., and Ferziger, J. H., 2003, "A Robust High-Order Compact Method for Large-Eddy Simulation," J. Comput. Phys., **191**(2), pp. 392–419.
[3] Morgan, P. E., Rizzetta, D. P., and Visbal, M. R., 2005, "Large-Eddy Simulation of Separation Control for Flow Over a Wall-Mounted Hump," AIAA Paper No. 2005-5017, June.
[4] Beaudan, P., and Moin, P., 1994, "Numerical Experiments on the Flow Past a Circular Cylinder at Sub-Critical Reynolds Number," Report TF-62, Department of Mechanical Engineering, Stanford University, Stanford, CA.
[5] You, D., Mittal, R., Wang, M., and Moin, P., 2004, "Computational Methodology for Large-Eddy Simulation of Tip-Clearance Flows," AIAA J., **42**(2), pp. 271–279.
[6] Choi, H., Moin, P., and Kim, J., 1992, "Turbulent Drag Reduction: Studies of Feedback Control and Flow Over Riblets," Report TF-55, Department of Mechanical Engineering, Stanford University, Stanford, CA.
[7] Tang, G., Yang, Z., and McGuirk, J. J., 2004, "Numerical Methods for Large-Eddy Simulation in General Co-Ordinates," Int. J. Numer. Methods Fluids, **46**(1), pp. 1–18.
[8] Kim, J., and Moin, P., 1985, "Application of a Fractional-Step Method to Incompressible Navier-Stokes Equations," J. Comput. Phys., **59**(2), pp. 308–323.
[9] Fadlun, E. A., Verzicco, R., Orlandi, P., and Mohd-Yusof, J., 2000, "Combined Immersed-Boundary Finite-Difference Methods for Three-Dimensional Complex Flow Simulations," J. Comput. Phys., **161**(1), pp. 35–60.
[10] Kim, J., Kim, D., and Choi, H., 2001, "An Immersed-Boundary Finite-Volume Method for Simulations of Flow in Complex Geometries," J. Comput. Phys., **171**(1), pp. 132–150.
[11] Piccirillo, P. S., and Van Atta, C. W., 1993, "An Experimental Study of Vortex Shedding Behind Linearly Tapered Cylinders at Low Reynolds Number," J. Fluid Mech., **246**, pp. 163–195.